31st Annual International Conference of the IEEE EMBS
Minneapolis, Minnesota, USA, September 2-6, 2009

A multi-level parcellation approach for brain functional connectivity analysis

Slim Karkar, Sylvain Faisan, Laurent Thoraval and Jack R. Foucher

***Abstract*— Most brain functional connectivity methods in fMRI require a brain parcellation into functionally homogeneous regions. In this work we propose a novel parcellation approach based on a spatial hierarchical clustering, that provides clusters within a multi-level framework. The method has the advantage of producing several brain parcellations rather than a single one from a fixed size-homogeneity criterion. Results obtained on real data demonstrate the relevance of the approach. Finally, a connectivity study shows the benefit of a prior multi-level parcellation of the brain.**

***Index Terms*— Functional Neuroimaging, Functional Connectivity, Parcellation, Hierarchical Clustering**

I. Introduction

Mapping of active brain regions remains a major objective of functional Magnetic Resonance Imaging (fMRI) studies. Another more recent and challenging one is the analysis of the overall brain dynamics. Following the definition of the functional connectivity by Friston [1], several approaches have been proposed to identify functional networks of interacting brain regions underlying cognitive functions. Most methods used in functional connectivity analysis search for significant links between a set of regions composed of spatially connected voxels. This set can be defined from *a priori* information, such as anatomical knowledge or activation studies. Another strategy, adopted in this paper, relies on a preliminary parcellation of the brain into functionally homogeneous regions([2], [3]).

Brain parcellation methods are based on a measurement that assesses parcel homogeneity (Pearson's correlation coefficient [2], coherence [4],...) and a clustering (or classification) method (e.g. fuzzy C-Means [5], region-growing [2]). Nonetheless, all methods have to deal with the same compromise between size and homogeneity of the clusters : partitioning the cortex into many (small) regions will lead to produce regions more homogeneous than those obtained using less (and larger) regions. The number of clusters can also be estimated using information theoretic criteria and cross-validation [6].

In this paper, rather than defining one flat partition of the brain into mutually exclusive (or disjoint) regions, a multi-level parcellation of the brain is proposed where a voxel could belong to several regions at a time : a (very) small region of (very) high homogeneity, and one or multiple larger regions of lower homogeneity for instance. The proposed parcellation method is based on a multi-level framework that produces at each level a new partition of the data.

S. Karkar, S. Faisan and L. Thoraval are affiliated to LSIIT/MIV (UMR 7005), CNRS, Université de Strasbourg karkar,faisan,thoraval@lsiit.u-strasbg.fr

Jack R. Foucher is affiliated to INSERM U666, Département de Psychiatrie, Centre Hospitalier Universitaire de Strasbourg

II. Methods

The multi-level parcellation algorithm consists in computing a series of dendrograms (a tree) (section II-A), from which a partition of the data is derived by thresholding (section II-B). The first dendrogram (level 1) is computed from the original data. The next ones (levels $i > 1$) are iteratively obtained from a cluster-based filtered version of the data (section II-C). The filtering process at level i is performed using the clusters obtained at level $i-1$. From level to level, the effect of filtering becomes more important, and clusters become larger. The overall procedure is depicted in Fig. 1.

A. Spatial hierarchical clustering

At each level, the procedure computes a dendrogram which is a top-down representation of the data : the root of the tree is composed of the whole set of voxels whereas each leaf represents a voxel, or equivalently a preprocessed time-series. The composition rule of the clusters is based on parental links : if node A is a parent of node B, the cluster associated with A *includes* the one associated with B. Finally, the vertical position of a node in a dendrogram reflects the homogeneity of its corresponding cluster. An example of a dendrogram is depicted in Fig. 1[a].

The computation of the dendogram is based on the hierarchical agglomerative algorithm (see [7]) : starting from the leaves, two elements (leaves or nodes) are grouped into one cluster if they have the closest distance among the set of distances of element pairs which can be grouped (an element pair may be grouped if each element has never been grouped during the procedure). Three distance measurements have also to be defined : a between voxel distance, a cluster-voxel distance, and a between cluster distance. The two last distances are named aggregation distances.

In our approach, the between voxel distance, D_{ij}, is based on the Pearson's correlation coefficient r_{ij} between the fMRI time series at voxels i and j : $D_{ij} = 1 - r_{ij}$. This distance represents the similarity between signals : it ranges from 0 (when $r_{ij} = 1$) to 2 (when $r_{ij} = -1$). For the two aggregation distances, several possibilities

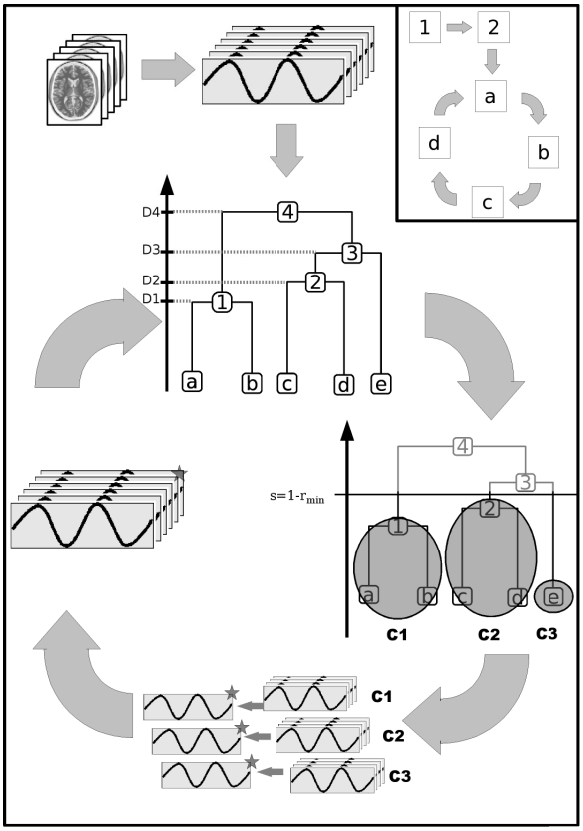

Fig. 1. *The brain multi-level parcellation procedure* : [1] fMRI data set, [2] data preprocessing, [a] construction of the dendrogram based on hierarchical clustering, [b] estimation of the clusters by FDR-based thresholding, [c] computation of the mean time-series for each cluster, [d] construction of the new data set from the mean time-series.

based on D_{ij} are offered (see [7]). Here, the farthest-neighbor method is used. It consists in selecting the maximal distance in the set of the involved distances so that *i)* the cluster-voxel distance between a voxel j and a cluster C is defined as : $D_{j,C} = \max_{k \in C}\{D_{j,k}\}$, and *ii)* the distance between clusters C_1 and C_2 is defined as :

$$D_{C_1,C_2} = \max_{j \in C_1} \max_{k \in C_2} D_{j,k}$$

It follows from this definition that the homogeneity of a region is guaranteed for a given distance. For example, when considering cluster C_3 in Fig. 1, the distance between two elements of C_3 cannot be greater than D_3.

Once distances are defined, the computation of a dendrogram is straightforward. However, to our knowledge, hierarchical clustering approaches do not usually account for spatial information. This could lead, in our case, to aggregate brain clusters or voxels that are not spatially connected. To cope with this problem, and guarantee the aggregation of connected clusters only, distances between non-neighboring elements are simply set to infinity, so that no links can be inferred between two voxels (or clusters) that are not spatially connected. Consequently, each node in the dendogram represents one connected component of the image.

B. Dendogram thresholding

Several approaches can be envisaged to infer a parcellation from a dendrogram (common methods are implemented in the Matlab Statistical Toolbox). In our approach, a minimal intra-cluster correlation r_{min} is guaranteed, by selecting, from the dendogram, clusters that present an aggregation distance inferior to the threshold $s = 1 - r_{min}$ and that are not included into a cluster exhibiting an aggregation distance inferior to s (see Fig. Fig. 1[b] for an example). The threshold s is computed thanks to the false discovery rate (FDR) defined, in our case, as the ratio of false aggregations to the number of aggregations. A false aggregation occurs when two voxels that do not belong to the same region are aggregated. The estimation of the FDR is performed numerically. First, the spatial hierarchical clustering algorithm described above is applied to a synthetic volume of randomly generated fMRI time-series, in order to obtain a dendrogram in which each aggregation accounts for a false aggregation. Then, for a given threshold s, the FDR is estimated by counting the number of aggregations obtained for s in the dendrogram associated to the real data and by estimating the expected number of false aggregations (under the threshold s) in the same dendrogram thanks to dendrograms obtained with synthetic data. The main difficulty to simulate fMRI data is to model properly the temporal and spatial correlations. In our case, a precise estimation of the FDR is not so crucial since the objective is to determine a subject-dependent threshold which only provides small significant regions (namely, regions which could be aggregated with other regions in other levels). Consequently, and for the sake of simplicity, fMRI signals were simulated as independent gaussian white noise.

C. Multi-level parcellation

As illustrated in Fig. 1, the spatial hierarchical clustering (step [a]) and the dendrogram thresholding (step [b]) are successively and iteratively performed to yield, at the output of each iteration, a new level of brain parcellation. For the first parcellation level, preprocessed fMRI signals are used as input data (step [2]). For the next ones, an adaptive cluster-based filering procedure is carried out (step [c] and [d]). More precisely, the signals composing each cluster of level $i-1$ are replaced by the mean signal of the cluster (step [c]). This filtered dataset is then used as a new input dataset for level i (step [d]). The multi-level parcellation steps are carried out until a final steady parcellation is reached, that is, when the brain parcellations of levels i and $i-1$ become identical.

Finally tone can easily notice that clusters become larger as iterations increase : if two regions R_i and R_j are obtained respectively at level i and j $(j > i)$, $R_j \cap R_i \neq \emptyset \iff R_i \subseteq R_j$, *i.e.* if one voxel from R_i belongs also to R_j, and $(j > i)$, then R_i is a subregion of R_j.

III. Experimental Results

A. fMRI data

The multi-level parcellation method was applied to real fMRI data acquired on a 2-T whole body S200 Bruker MRI system with a head volume coil, using echo-planar imaging (EPI) with an axial slice orientation. In this study, 7 subjects were asked to perform event-related working memory tasks. For each subject, 6 sequences of 158 3-D scans were acquired ($64 \times 64 \times 28$ voxels, voxel size : $4 \times 4 \times 4mm$, TE/TR : 43 ms/2.9 s).

Prior to the parcellation, the 6 fMRI scan sequences associated to a subject were processed separately using the following steps : registration of all scans to the first scan, movement and physiological noise correction using an ICA procedure, trend removal using second order polynomial fit, temporal bandpass filter with a passband of 0.001 to 0.1 Hz, normalization of the fMRI signal (unit variance). Then, a single sequence of 6 x 158 fMRI scans was derived for each of the seven proceeded subjects by registering the mean fMRI scans associated to each sequence. A segmentation procedure was finally used to keep the voxels corresponding to the gray matter.

B. Activation study

In order to highlight our multi-level parcellation approach, a brain functional activation study was conducted within the general framework of SPM (www.fil.ion.ucl.ac.uk/spm). The objective was to compare the influence of the cluster-based filtering used in our parcellation procedure with respect to the Gaussian spatial filtering traditionaly used in SPM. To this end, and for each of the seven subjects, standard fixed-effects activation studies were performed using SPM5 from 6 different datasets. The first data set, DS0, was obtained at the output of the preprocessing step, that is, without any spatial filtering. Then, two spatially filtered versions of DS0, denoted DSG6 and DSG8, were obtained by applying Gaussian spatial smoothing to DS0 with FWHM (Full Width at Half Mean) of 6 mm for DSG6, and of 8 mm for DSG8. Finally, for comparison purposes, three cluster-based filtered versions of DS0, namely DSL1, DSL2, and DSL3, were considered, each one corresponding to the level 1, level 2, and level 3 of parcellation of DS0, respectively.

An illustrative example of the obtained results is represented in Fig. 2. It shows in a lexicographic order, an axial section of the $t-test$ activation maps obtained with the data sets DS0, DSG6, DSG8, DSL1, DSL2, and DSL3. To facilitate their analysis, the $t-test$ maps illustrated in Fig. 2 are visualized before thresholding.

The results obtained without spatial filtering (Fig. 2(A)) are not satisfactory since only a few voxels have a significant t-test value (21 voxels present a t-test value greater than 3). When Gaussian spatial prefiltering of the data is used (Fig. 2(B,C)), results are clearly improved (resp. 36 and 91 voxels have a t-test value greater than 3). Though the Gaussian spatial filtering reduces noise while increasing the significance of the activated voxels, this kind of filtering suffers from a major well-known limitation illustrated in Fig. 2(C) : it tends to blur the activated area (see the upper right panel), while limiting the precision of their localization. In extreme blurring conditions, two activated areas separated by a small distance *w.r.t.* the FWHM can be grouped into one single region, or a small activated area *w.r.t.* the FWHM may not be detected.

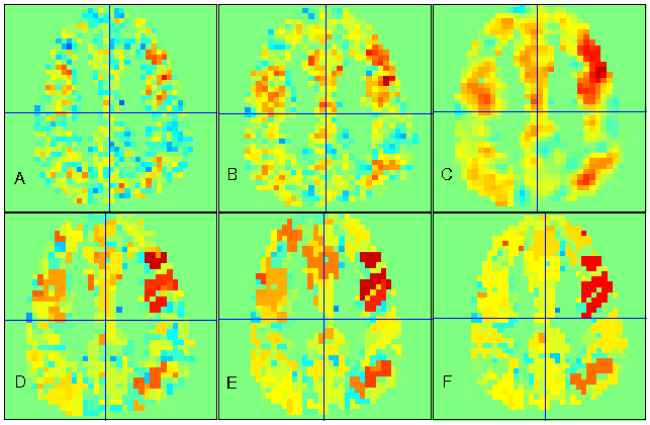

Fig. 2. $t-test$ maps of a representative subject obtained using SPM5 with : (A) the non-spatially-filtered dataset DS0, (B,C) the Gaussian filtered data sets DSG6 (FWHM=6mm) and DSG8 (FWHM=8mm, (D,E,F) the cluster-based filtered data sets DSL1, DSL2, and DSL3 (see text).

In contrast, our multi-level parcellation approach blurs less activated areas. In particular, the upper right panel of Fig. 2(E, F) shows two activated areas whereas a unique activated area is observed in the corresponding panel of Fig. 2(C). On first analysis, one could attribute this result to an underdetection of activation, but activation maps obtained with our approcach exhibit much more significant voxels (resp. 57, 151 and 357 for DSL1, DSL2 and DSL3). More generally, when considering all subjects, the mean amount of significant voxels (t-test value > 3) is resp. of 21, 82, and 162 voxels for the datasets DS0, DSG6 and DSG8. With the multi-level parcellation approach, those amounts are increased resp. to 85, 152 and 291 for the datasets DSL1, DSL2 and DSL3. These good results demonstrate that the cluster-based filtering used in the multi-level parcellation approach takes better into account spatial information, essentially because it is applied to delimited homogeneous area.

Fig. 2(D,E,F) also shows some activated regions that appear or disappear across levels. The former phenomenon can be explained by the fact that merging *a priori* inactive clusters could enhance the mean activity of the resulting cluster by noise reduction. The latter phenomenon can be explained by the merging of active clusters with inactive or less active voxels, which tends to reduce the mean activity of the resulting cluster. Both phenomena demonstrate the interest of a multi-level brain parcellation rather than one flat partition.

Finally the images obtained by surperimposing parcels

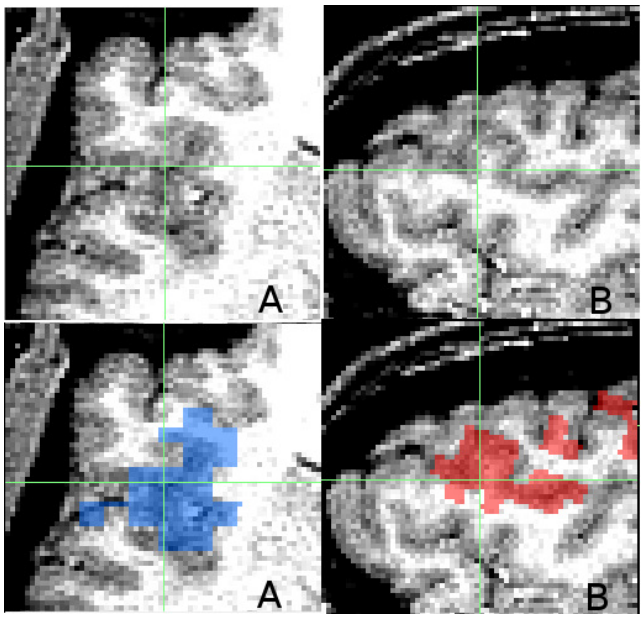

Fig. 3. Illustrative regions obtained with the parcellation process (2 regions, A and B). Top : axial and sagital sections of the anatomical scan. Bottom : two regions (red or blue) obtained by the proposed approach.

on anatomical scans demonstrate in many ways the validity of the clustering approach. First the cluster shape fits the brain anatomy : many clusters follow the shape of a sulcus which can be considered as functionally homogeneous at least at the resolution allowed by our data. Second, the locations of the significant clusters are usually in good agreement with the stimulation paradigm used (verbal working memory) : left inferior frontal sulcus (Fig. 3(B)) or the Sylvian sulcus (Fig. 3(A)). Finally, a sharp contrast is observed between the significance of the relevant cluster and its surroundings, in accordance with the functional segregation of function in the brain.

C. Towards functional connectivity

This last experiment illustrates, in a prospective manner, how a functional network can be derived from a multi-level brain parcellation. To this end, clusters of a size of less than 60 or greater than 600 voxels are neglected because they are physiologically inappropriate. Then, only links between disjoint clusters are considered. Applied to the previous case study, these two criteria lead to a total of 10987 possible links between 151 brain parcels. Note here that despite multiple parcellation levels used to investigate brain functional connectivity, the number of potential links to handle remains tractable. Since we search for networks of clusters for which the neural activities show interactions related to the cognitive tasks, the measurement of an interaction between two clusters is computed as the Pearson's correlation coefficient of their representative fMRI time-series, weighted by the paradigm. Finally, significant links with a non-corrected p-value of 10^{-5} are retained (this p-value is estimated as previously by simulating fMRI signals). The resulting functional network is depicted in Fig. 4.

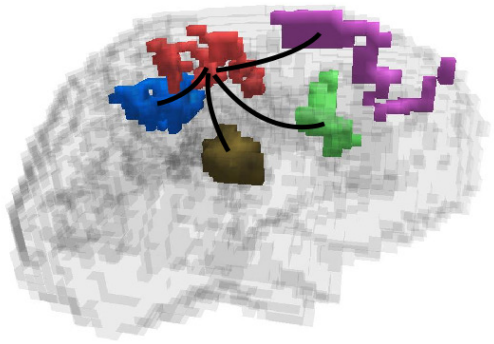

Fig. 4. 3-D representation of the functional network, regions colors are set arbitrary

It is composed of 5 brain regions issued from 3 distinct parcellation levels, namely the first three ones. Similar results were obtained for the six other subjects. Though their neurocognitive interpreation is still under progress, these preliminary results demonstrate the relevance of a multi-level parcellation of the brain.

IV. Conclusion

A new parcellation approach has been proposed within the context of functional brain connectivity analysis. In this approach, the size-homogeneity compromise is relaxed within a multi-level framework by yielding several levels of brain parcellation rather than a unique one. Moreover, the Gaussian spatial filtering traditionally applied to the raw fMRI data is replaced by an adaptive, and iterative "cluster-based" smoothing that prevents the traditional blurring effects.

References

[1] K.J. Friston, "Functional and effective connectivity in neuroimaging : a synthesis," *Hum. Brain Mapp.*, vol. 2, pp. 56–78, 1994.

[2] P. Bellec, V. Perlbarg, S. Jbabdi, M. Pelegrini-Issac, J. Antonand J. Doyon, and H. Benali, "Identification of large-scale networks in the brain using fMRI," *NeuroImage*, vol. 29, pp. 1231–1243, 2006.

[3] B. Thirion, D. Silke, and J. B. Poline, "Detection of signal synchronizations in resting-state fMRI datasets," *NeuroImage*, vol. 29, no. 1, pp. 321–327, 2006.

[4] K. Müller, J. Neumann, M. Grisgutsch, Y. von Cramon, and G. Lohmann, "Detecting groups of coherent voxels in functional MRI data using spectral coherence and replicator dynamics," *Magn Reson Imaging*, vol. 26, pp. 2642–2650, 2007.

[5] B. Thirion, G. Flandin, P. Pinel, A. Roche, P. Ciuciu, and Poline J. B., "Dealing with the shortcomings of spatial normalization : multi-subject parcellation of fMRI datasets.," *Hum. Brain Mapp.*, vol. 27, no. 8, pp. 678–93, 2006.

[6] B. Thyreau, G. Flandin, and J. B. Poline, "Anatomo-functional description of the brain : a probabilistic approach," in *In : Proceedings of the 2006 International Conference on Acoustics, Speech and Signal Processing ICASSP 2006*, 2006.

[7] R. O. Duda, P. E. Hart, and D. G. Stork, *Pattern Classification (2nd Edition)*, Wiley-Interscience, 2000.